ELSEVIER

12 November 2001

Physics Letters A 290 (2001) 139–144

PHYSICS LETTERS A

www.elsevier.com/locate/pla

Chaos–hyperchaos transition in coupled Rössler systems

S. Yanchuk [a], T. Kapitaniak [b,*]

[a] *Institute of Mathematics, Academy of Sciences of Ukraine, 3 Tereshchenkivska st, Kiev 01601, Ukraine*
[b] *Division of Dynamics, Technical University of Lodz, Stefanowskiego 1/15, 90-924 Lodz, Poland*

Received 26 February 2001; received in revised form 7 May 2001; accepted 27 September 2001
Communicated by A.P. Fordy

Abstract

Many of the nonlinear high-dimensional systems have hyperchaotic attractors. Typical trajectory on such attractors is characterized by at least two positive Lyapunov exponents. We provide numerical evidence that chaos–hyperchaos transition in six-dimensional dynamical system given by flow can be characterized by the set of infinite number of unstable periodic orbits embedded in the attractor as it was previously shown for the case of two coupled discrete maps.

PACS: 05.45.+b

1. Introduction

Unstable periodic orbits (UPO's) constitute the most fundamental blocks of a chaotic system [1]. Theoretically, the infinite number of UPO's embedded in a chaotic set provides the skeleton of the attractor and allows the estimation of many dynamical invariants such as the natural measure, the spectra of Lyapunov exponents, the fractal dimension in the fundamental way [2]. Recently, UPO's have been used in the description of higher-dimensional dynamical phenomena such as blowout bifurcation [3] and chaos–hyperchaos transition (i.e., transition from the attractor characterized by one positive Lyapunov exponent to the attractor characterized by at least two positive exponents) [4]. It has been shown that chaos–hyperchaos transition as well as blowout bifurcation is mediated by an infinite number of UPO's which become repellers in the neighborhood of the transition point. The simultaneous existence of UPO's with different number of unstable direction gives rise to the nonhyperbolicity known as unstable dimension variability and provides a possible dynamic mechanism for the smooth transition through zero of second Lyapunov exponent.

Up to now, the description of chaos–hyperchaos transition using UPO's has been performed only for the case of coupled discrete maps. In this Letter, we argue and provide numerical evidence that this description can be applied to the continuous dynamical systems (flows). We show that the balance of the appropriate weights of UPO's orbits with one unstable dimension and UPO's with at least two unstable dimension gives the approximation of chaos–hyperchaos transition point.

2. The model

As an example consider two identical symmetrically coupled Rössler systems

* Corresponding author.
E-mail address: tomaszka@ck-sg.p.lodz.pl (T. Kapitaniak).

0375-9601/01/$ – see front matter
PII: S0375-9601(01)00651-X

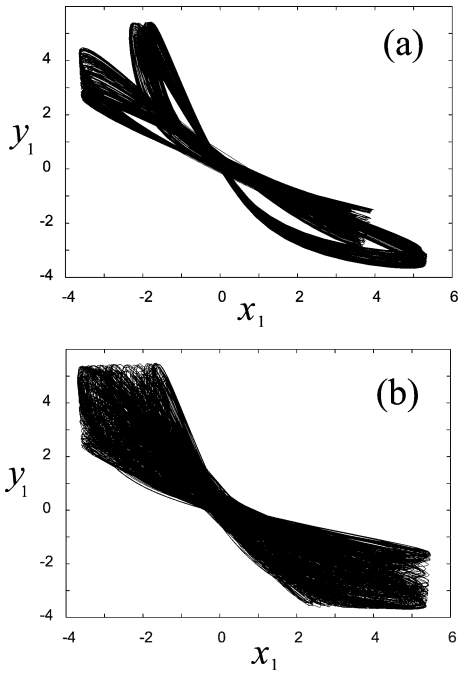

Fig. 1. Two-dimensional projections onto (x_1, y_1) plane of the attractor in system (1): (a) chaotic, $a = 0.363$; (b) hyperchaotic, $a = 0.368$.

$$\begin{aligned}
\dot{x}_1 &= -x_2 - x_3,\\
\dot{x}_2 &= x_1 + ax_2,\\
\dot{x}_3 &= b + x_3(x_1 - c) + d(y_3 - x_3),
\end{aligned} \tag{1}$$

$$\begin{aligned}
\dot{y}_1 &= -y_2 - y_3,\\
\dot{y}_2 &= y_1 + ay_2,\\
\dot{y}_3 &= b + y_3(y_1 - c) + d(y_3 - x_3),
\end{aligned}$$

where $(x_1, x_2, x_3, y_1, y_2, y_3) \in \mathcal{R}^6$ are dynamical variables, a, b, c are system parameters and d is the coefficient of coupling. It is well known that the Rössler system develops continuous chaos through period-doubling bifurcation cascade [6]. Since the Rössler system has a foundation in the kinematics of chemical reaction [7], it is natural to study the diffusive coupling of two such systems [8].

In our numerical studies we took the following parameter values $b = 2.0$, $c = 4.0$, $d = 0.25$ and consider a as a control parameter. With the increase of the control parameter a, system (1) reveals the transition to hyperchaos [8] with a smooth passing of the second Lyapunov exponent through zero at $a = a_h$. An

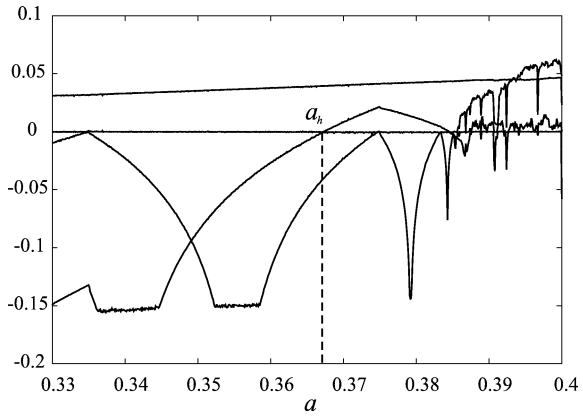

Fig. 2. The variation of three largest Lyapunov exponents for the coupled Rössler system (1) for $d = 0.25$. The smooth transition to hyperchaos occurs at $a_h \approx 0.3673$.

examples of chaotic attractors (two-dimensional projections) are shown in Figs. 1(a) and (b). The attractor calculated for $a = 0.363$ is shown in Fig. 1(a). It is "two-bundle" chaotic set with one positive Lyapunov exponent $\lambda_1 \approx 0.039$. Fig. 1(b) shows the apparently symmetrical attractor which exists for $a = 0.368$ and has two positive Lyapunov exponents $\lambda_1 \approx 0.040$ and $\lambda_1 \approx 0.002$. Both attractors are not located in the invariant manifold $x = y$.

The variation of three Lyapunov exponents versus a is shown in Fig. 2 (for system (1) one of Lyapunov exponents is always equal to zero). One can observe a typical smooth transition to hyperchaos (similar to this observed in [9,10]) at $a_h \approx 0.3673$. For the calculation of Lyapunov exponents we integrate the original as well as a set of linearized equations and reorthonormalize the difference vectors periodically using a modified Gram–Schmidt algorithm (see [5] and references therein).

Ordinary differential equations (1) have been solved numerically using the fourth-order Runge–Kutta method. The standard discretization of the time derivatives in (1) allows the replacement of the original set of ordinary differential equations by the corresponding discrete map. Chaos–hyperchaos transition at a_h is a topological event which is independent of the applied discretization method and integration step. This allows one to expect that the same mechanism of chaos–hyperchaos transition which is known for two coupled maps [4], can be observed in the discrete map associ-

ated with Eqs. (1). Due to the problems of calculation of unstable periodic orbits embedded in chaotic and hyperchaotic attractors of higher- (larger than two) dimensional maps the extension of the results of [4] to system (1) is not straightforward and this is the main motivation of the current study.

3. Stability of low-periodic orbits embedded into the attractor

In the following, we try to investigate stability of low-periodic orbits embedded into the attractor of system (1) when it undergoes chaos–hyperchaos transition. In order to find and classify these orbits we use the Poincaré cross-section that is determined by the following normal vector $\mathbf{n} = (-3.75, 1.84, -6.48, 1.75, -2.09, -0.10)$ and a base point with coordinates $P = (1.72, 0.35, 3.40, -1.27, -2.29, 0.53)$. Vector $\mathbf{n}$ was chosen along flow (1) at point P. Fig. 3 shows the image of the chaotic attractor in this map for $a = 0.363$. Note that system (1) has additionally a symmetric attractor which can be obtained by replacing x with y.

In order to discover what periods of periodic solutions are admitted for the given Poincaré map, we shall consider symbolic dynamics of the map. It appears that it changes when the control parameter is increased. Figs. 4(a) and (b) show possible cases. In the first case we can split the phase space onto two nonintersecting regions A and B that maps into each other: $A \to B$ and $B \to A$. Since we may obtain the only possible periodic solutions, which correspond to symbolic sequences $ABAB\ldots$, and have even peri-

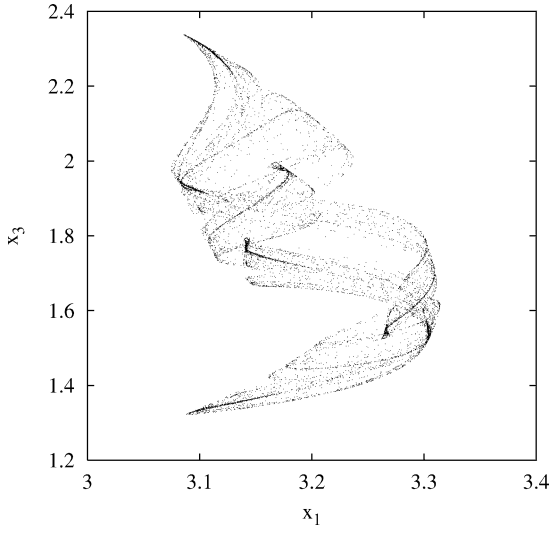

Fig. 3. 2D projection of the Poincaré map of system (1) onto the plane (x_1, x_3), $a = 0.363$ (only one piece of two-piece attractor is shown).

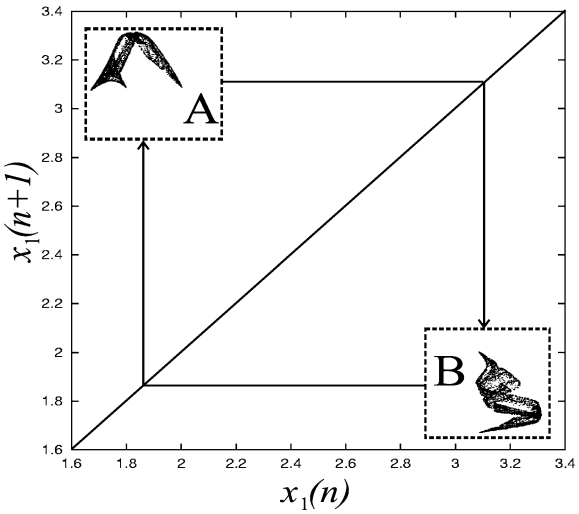

(a)

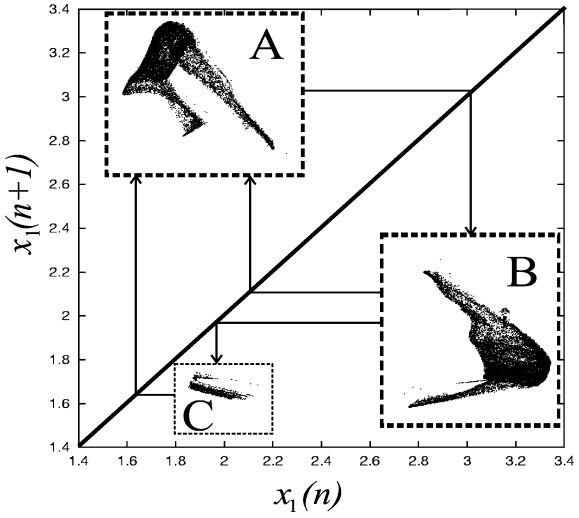

(b)

Fig. 4. Map $x_1(n+1)$ versus $x_1(n)$ constructed for the Poincaré map considered in Section 3: (a) $a = 0.363$; (b) $a = 0.36713$. A, B, and C are domains in the phase space that represent possible partitions.

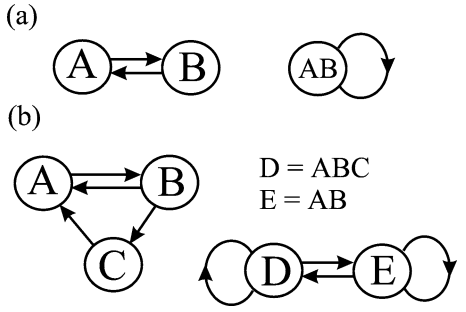

Fig. 5. Graphs that are related to the symbolic dynamics in system (1) with respect to the Poincaré map considered in Section 3: (a) $a = 0.363$; (b) $a = 0.0.36713$.

ods $2n$ for any natural n. The attractor in this case has a form of two-bundle set shown in Fig. 1(a). With the increase of parameter a the shape of the attractor changes and it begins to intersect the Poincaré map at a new set of points. Thus, the topological structure of the invariant set for the discrete map in the cross-section changes, and we may observe also periodic cycles with odd periods. With increasing parameter a we may observe also the periodic cycles with odd periods. More precisely, the symbolic dynamics now can be constructed with the use of the partition $\{A, B, C\}$, cf. Fig. 4(b). Possible motions between the partitions are $A \to B$, $B \to A$, $B \to C$, and $C \to A$. The corresponding graph is shown in Fig. 5(b). Minimal alphabet in this case may be chosen, for example, as consisting of two letters $D = ABC$ and $E = AB$. Thus, we obtain fully connected graph, cf. Fig. 5(b). Therefore, the admissible periodic cycles will correspond to all symbolic sequences which consist of the letters D and E. Since letter D corresponds to three iterations of the Poincaré map, and C to two iterations, the following periods for the map are allowed: $p = 3n + 2m$, where m, and n are natural numbers, $n + m \neq 0$, i.e., $p > 1$.

Having found the admissible periods p, we applied the shooting method [5,12] for locating periodic orbits of system (1) first getting the initial guess by iterating pth power of the Poincaré map. The periods $p \leqslant 24$ were investigated. Let γ_i^p be a period-p orbit and ν_1, ν_2 be the largest multipliers of this orbit. Here i is an index labeling the orbit. Then $\lambda_1 = \ln(\nu_1)/T$ and $\lambda_2 = \ln(\nu_2)/T$ are the first two largest Lyapunov exponents of the corresponding orbit of system (1) of a period T. Figs. 6(a) and (b) show the second Lyapunov exponents $\lambda_2(\gamma_i^p, p)$ of the found orbits versus p for two values of the control parameter: $a_1 = 0.364$ and $a_2 = 0.367$. The first value of the parameter was chosen just after the moment when we first observe doubly unstable low-periodic orbit embedded into the attractor (we assumed that this bifurcation occurs at $a = a_r$), i.e., $a_1 \gtrsim a_r$, while the second one is $a_2 \lesssim a_h$. It can be seen that the number of doubly unstable orbits increases and the number of cycles with one unstable multiplier decreases when one approaches chaos–hyperchaos point a_h.

More precise characteristic may be obtained by calculating weights $\Lambda_p^2(a)$ and $\Lambda_p^1(a)$ that correspond to doubly unstable cycles and the cycles with one unstable multiplier, respectively, cf. [3,4,11]. They are defined as follows:

$$\Lambda_p^1 = \sum_{i=1}^{N_p^1} \rho\bigl(\gamma_i^p, p\bigr)\lambda_2'\bigl(\gamma_i^p, p\bigr),$$

$$\Lambda_p^2 = \sum_{i=1}^{N_p^2} \rho\bigl(\gamma_i^p, p\bigr)\lambda_2'\bigl(\gamma_i^p, p\bigr),$$

where N_p^1 and N_p^2 are the numbers of cycles that have one and two unstable directions, respectively. The cycle γ_i^p weight is [13]

$$\rho\bigl(\gamma_i^p, p\bigr) = p\frac{L_i^{-1}}{\sum_{i=1}^{N_p^1+N_p^2} L_i^{-1}}, \tag{2}$$

where L_i is the product of the unstable multipliers of ith cycle, i.e., either $L_i = \nu_1$ or $L_i = \nu_1\nu_2$ in the case of a doubly unstable cycle. $\lambda_2'(\gamma_i^p, p) = (1/p) \times \ln \nu_2(\gamma_i^p, p)$ is the second Lyapunov exponent of a periodic orbit γ_i^p for the Poincaré map.

Following to [3], the zero value of the quantity $\Delta\Lambda_p(a) = \Lambda_p^1 + \Lambda_p^2$ may serve as an approximation of the blowout bifurcation point for the attractors in invariant subspace. By the analogy to that approach and [4] we may approximate the chaos–hyperchaos transition point. Figs. 7(a)–(c) show variation of $\Delta\Lambda_p(a)$ with a for p equal to 12, 20 and 24. For all parameter values from 1000 to 2000 fixed points of pth power of the Poincaré map were accumulated. Although we cannot affirm that all periodic orbits up to period p are calculated, Fig. 7 shows clearly

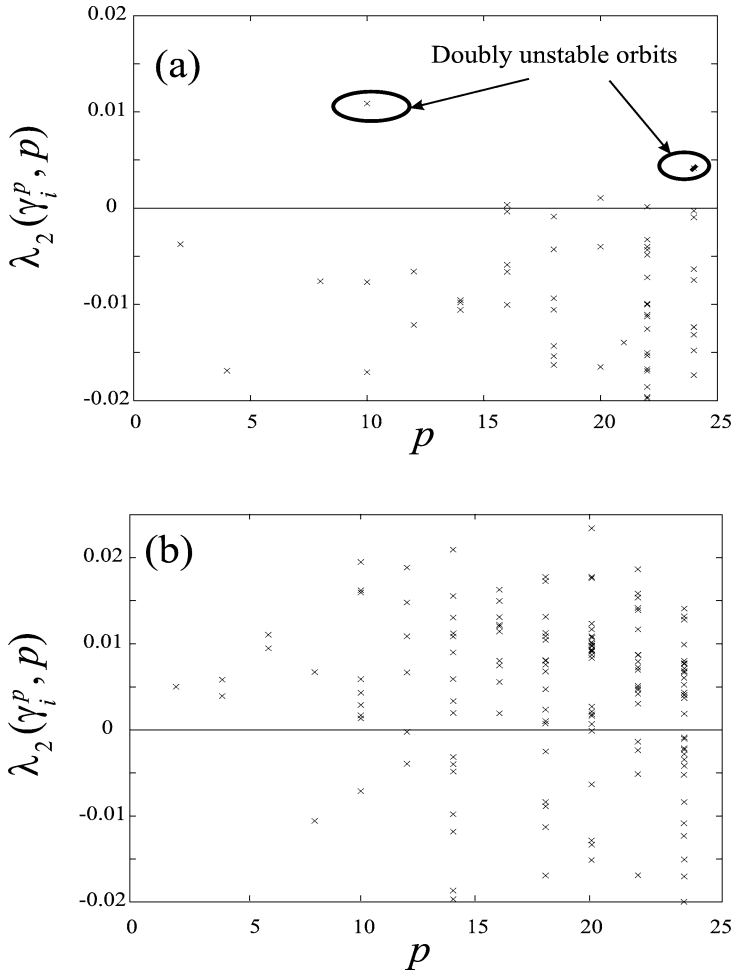

Fig. 6. The second Lyapunov exponent $\lambda_2(\gamma_i^p, p)$ for low-periodic orbits embedded into the attractor of system (1) versus p: (a) $a = 0.365$; (b) $a = 0.367$.

that approximately the same value of the weights Λ_p^1 and Λ_p^2 occurs near the chaos–hyperchaos transition point. This is specially visible as one considers the mean square approximation of $\Delta\Lambda_p(a)$ shown in a broken line. One can find that calculations for $p = 24$ (Fig. 7(c)) give better approximation of chaos–hyperchaos transition point a_h than calculations for $p = 20$ (Fig. 7(b)) and $p = 12$ (Fig. 7(a)). Note that the fluctuations of $\Delta\Lambda_p(a)$ around zero before chaos–hyperchaos transition which can be observed for larger p ($p = 20$ (Fig. 7(b)) and $p = 12$ (Fig. 7(a))) are due to the finite number of considered UPO's. We observed that increasing p these fluctuations decrease.

4. Conclusions

We have shown here that the transition from chaos to hyperchaos in higher-dimensional dynamical system given by a flow is a bifurcation that like in the case of the coupled maps, is mediated by an infinite number of unstable periodic orbits. In the neighborhood of the transition point one observes the co-existence of UPO's with one (saddles which are typical for 3-dimensional chaotic systems) and at least two unstable eigenvalues. This co-existence is responsible for the occurrence of nonhyperbolic behaviour known as unstable dimension variability and can explain the

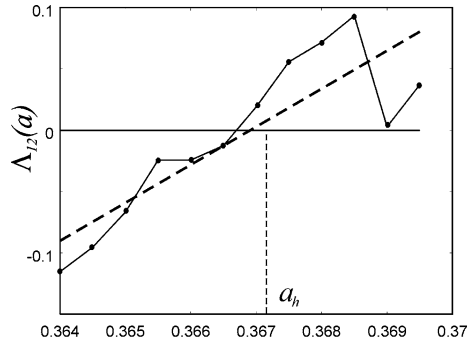

(a)

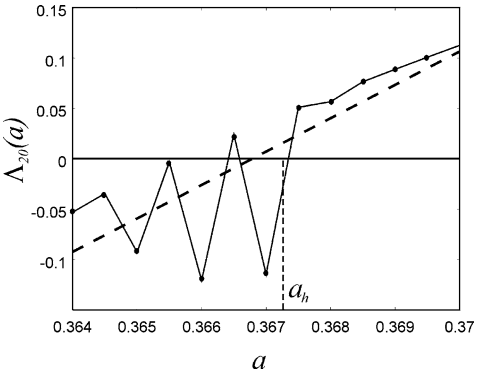

(b)

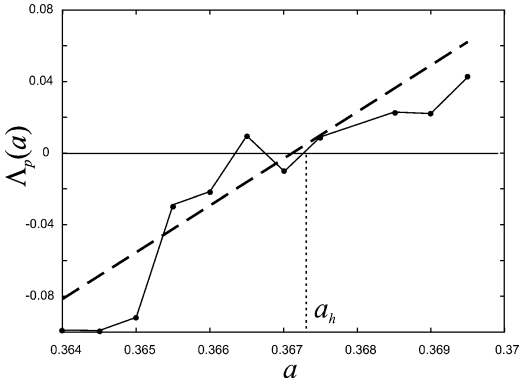

(c)

Fig. 7. Variation of $\Lambda_p(a)$ for (a) $p = 12$, (b) $p = 20$, and (c) $p = 24$. The approximation of the chaos–hyperchaos transition point by low-periodic orbits up to period $p = 12, 20, 24$, the broken lines show the mean-square approximations.

smooth passage through zero of the second Lyapunov exponent at chaos–hyperchaos transition point. In a system given by a flow despite the fact that it is impossible to determine all UPO's of the given period the balance of the appropriate weights of UPO's of different types can approximate the transition point in the control parameter space.

References

[1] D. Auerbach, P. Cvitanovic, J.-P. Eckmann, G.H. Gunaratne, I. Procaccia, Phys. Rev. Lett. 58 (1987) 2387;
G.H. Gunaratne, I. Procaccia, Phys. Rev. Lett. 59 (1987) 1377;
P. Cvitanovic, Chaos 2 (1992) 1.
[2] C. Grebogi, E. Ott, J.A. Yorke, Phys. Rev. A 37 (1988) 1711;
Y.C. Lai, Y. Nogai, C. Grebogi, Phys. Rev. Lett. 79 (1997) 649.
[3] Y. Nagai, Y.-C. Lai, Phys. Rev. E 55 (1997) R1251;
Y. Nagai, Y.-C. Lai, Phys. Rev. E 56 (1997) 4031;
Y.-C. Lai, Phys. Rev. E 59 (1999) R3803.
[4] T. Kapitaniak, Yu. Maistrenko, S. Popovich, Phys. Rev. E 62 (2000) 1972.
[5] T.S. Parker, L.O. Chua, Practical Numerical Algorithms for Chaotic Systems, Springer, New York, 1989.
[6] O.E. Rössler, Phys. Lett. A 57 (397) 1976.
[7] O.E. Rössler, Z. Naturfosch. 31A (1976) 259.
[8] J. Rasmussen, E. Mosekilde, C. Reick, Math. Comp. Sim. 40 (1996) 247.
[9] T. Kapitaniak, Phys. Rev. E 47 (1993) R2975.
[10] M.A. Harrison, Y.-C. Lai, Phys. Rev. E 59 (1999) 3803.
[11] Y.-C. Lai, Phys. Rev. E 56 (1997) 1407.
[12] A.J. Mees, Dynamics of Feedback Systems, Wiley, New York, 1981.
[13] C. Grebogi, E. Ott, J.A. Yorke, Phys. Rev. A 37 (1988) 1711.